Regular Article

Nuclear Expression of Pygo2 Correlates with Poorly Differentiated State Involving c-Myc, PCNA and Bcl9 in Myanmar Hepatocellular Carcinoma

Myo Win Htun[1], Yasuaki Shibata[1], Kyaw Soe[2] and Takehiko Koji[1,3]

[1]Department of Histology and Cell Biology, Nagasaki University Graduate School of Biomedical Sciences, Nagasaki 852–8523, Japan, [2]Department of Medical Research, Yangon, 11191, Myanmar and [3]Office for Research Initiative and Development, Nagasaki University, Nagasaki 852–8521, Japan

In Myanmar, hepatocellular carcinoma (HCC) is commonly seen in young adult and associated with poor prognosis, while the molecular mechanisms that characterize HCC in Myanmar are unknown. As co-activation of Wnt/β-catenin signaling and c-Myc (Myc) are reported to associate with malignancy of HCC, we immunohistochemically investigated the expression of Pygo2 and Bcl9, the co-activators of the Wnt/β-catenin signaling, Myc and PCNA in 60 cases of Myanmar HCC. Pygo2 expression was confirmed by *in situ* hybridization. The signal intensity was measured by image analyzer and then statistically analyzed. As a result, the expression of Pygo2 was significantly higher in HCC compared to normal liver tissue and the nuclear signal was the most intense in poorly differentiated HCC. Cytoplasmic Bcl9 was expressed in the normal liver tissue but decreased in HCC with the progression of histopathological grade. Myc was significantly higher in poorly differentiated HCC, whereas PCNA labeling index increased with the progression of histopathological grade. Nuclear Pygo2 showed strong correlation with nuclear Myc (*P* < 0.01) and PCNA (*P* < 0.001), and inversely correlated with cytoplasmic Bcl9 (*P* < 0.01). Our results suggested Wnt/β-catenin and Myc signaling is commonly activated in Myanmar HCC and that the correlative upregulation of nuclear Pygo2 and Myc characterizes the malignant features of HCC in Myanmar.

Key words: Pygo2, Bcl9, c-Myc, PCNA, Myanmar hepatocellular carcinoma

I. Introduction

Hepatocellular carcinoma (HCC) is the sixth most common cancer worldwide and the third leading cause of cancer-related mortality in the Asia-Pacific region [23, 59]. In Myanmar, the rates of liver cancer increase after 20 years of age and reach a peak at the age of 50 years, whereas in Japan, the incidence of liver cancer increases after the age of 45–50 years and reaches a plateau around 65 years of age [5]. These data suggest that certain signaling dysregulation that accelerates the development and progression of HCC seems to occur in Myanmar HCC. One of the factors considered to enhance the development and progression of Myanmar HCC is excess iron uptake and its heavy deposition in the liver [40, 48], while the signaling that characterize poor prognosis of Myanmar HCC are unknown yet.

Deregulation of the canonical Wnt/β-catenin signaling pathway associated with overexpression and mutation of the molecules associated with the signaling, such as β-catenin and Axin, was found to play a role in the development and progression of HCC [15, 30, 34, 51]. In the absence of Wnt ligands, β-catenin is phosphorylated and degraded by a destruction complex comprising adenomatous polyposis coli (APC), Axin, glycogen synthase kinase-3β and casein kinase 1α. The presence of the ligand, however, disrupts the destruction complex, allowing the unphosphorylated β-catenin to be translocated into

Correspondence to: Associate Professor Yasuaki Shibata, D. D. S., Ph.D., Department of Histology and Cell Biology, Nagasaki University Graduate School of Biomedical Sciences, 1–12–4, Sakamoto, Nagasaki 852–8523, Japan. E-mail: siva@nagasaki-u.ac.jp

the nucleus. Then, nuclear β-catenin binds to members of the T-cell factor/lymphoid enhancer factor (TCF/LEF) family to drive a Wnt transcriptional program [11, 17, 25, 46]. In addition, for activation of the pathway, simultaneous nuclear translocation of Pygo2 and Bcl9 other than β-catenin is indispensable. Pygo2 that has a nuclear localization sequence (NLS) in its N-terminus, binds to Bcl9, followed by translocation to the nucleus [29]. In the nucleus, Pygo2 binds to β-catenin via Bcl9 and is suggested to recruit β-catenin complex to activate chromatin through its interaction with trimethylated lysine 4 residues of histone H3 to regulate the proliferation of mammary cells [38].

Previous studies reported that aberrant expression or nuclear localization of Pygo2 or Bcl9 correlates with poor HCC prognosis [18, 19, 39, 58]. Our group had also demonstrated the expression of Bcl9 in the cytoplasm even in the normal liver tissue, while the expression is significantly decreased during the progression of histopathological grade and also in juvenile HCC in Myanmar [41]. The gradual loss of cytoplasmic Bcl9 along with the progression of HCC suggests the association of Pygo2 not only in poorly differentiated HCC but also in most of Myanmar HCC by inducing nuclear translocation of Bcl9 followed by activation of Wnt/β-catenin signaling.

Deregulation of Myc gene is the driving force in the majority of human cancers [1, 43]. There is growing evidence that both Myc and Wnt/β-catenin signaling pathways are activated in HCC patients with poor prognosis; Myc amplification tended to co-occur with CTNNB1 (encoding β-catenin) mutations in HCC [14]. Myc-driven HCC frequently acquired activating mutations of CTNNB1 [6, 56]. Especially, activation of Wnt/β-catenin signaling accelerated Myc-driven carcinogenesis in mouse liver [4].

In the present study, we hypothesized that simultaneous activation of Wnt/β-catenin signaling and Myc characterize malignant features of HCC in Myanmar. To test the hypothesis, we used immunohistochemistry for Pygo2, Bcl9, Myc and PCNA on serial paraffin sections of Myanmar HCC. We also examined the expression Pygo2 mRNA by *in situ* hybridization. The cytoplasmic and nuclear signal intensities of immunohistochemistry were further determined by measuring with image analyzer and statistically compared the normal liver tissue and each histopathological grade of Myanmar HCC. Finally, we performed correlation analysis of each signal intensity.

II.   Materials and Methods

Chemicals and antibodies

3-Aminopropyltriethoxysilane (APS), proteinase K, bovine serum albumin (BSA, minimum 98%, electrophoresis), yeast transfer RNA (type X-SA), salmon testes DNA, dextran sulfate, 30% Brij® L23 solution were purchased from Sigma Chemical Co. (St Louis, MO, USA). Formamide (nuclease and protease free)

was purchased from Nacalai Tesque (Kyoto, Japan). Digoxigenin-11-dUTP and terminal deoxynucleotidyl transferase (TdT) were from Roche (Mannheim, Germany). 3,3'-Diaminobenzidine-4HCl (DAB) was bought from Dojin Chemical Co. (Kumamoto, Japan). Permount was obtained from Thermo Fisher Scientific (Hudson, NH, USA). The oligodeoxynucleotides used for *in situ* hybridization were obtained from Life Technologies (Carlsbad, CA, USA). All other reagents used in this study were from Wako Pure Chemicals (Osaka, Japan) and of analytical grade.

Antibodies used in this study were as follow: Mouse monoclonal Pygopus 2 antibody (concentration; 4 μg/ml, sc-390506, Santa Cruz Biotechnology, Inc., Santa Cruz, CA, USA), mouse monoclonal anti-human Bcl9 antibody (concentration; 4 μg/ml, Bio Matrix Research Inc., Tokyo, Japan), mouse monoclonal Myc antibody (concentration; 5 μg/ml, OM-11-906, Cambridge Research Biochemicals, UK), mouse monoclonal anti-proliferating cell nuclear antigen antibody (concentration; 2.6 μg/ml, Clone PC 10, DAKOCytomation, Glostrup, Denmark), Normal mouse IgG (DAKO, Glostrup, Denmark) was used instead of each primary antibody at concentration similar to each primary antibody. HRP-goat anti-mouse IgG (concentration; 5 μg/ml, Millipore, Temecula, CA, USA) and HRP-conjugated goat anti-digoxigenin antibody (concentration; 5 μg/ml, Roche, Indianapolis, IN, USA) were used as secondary antibodies. All antibodies were validated by each supplier using immunohistochemistry and/or western blotting.

Clinical tissue samples

The cancerous liver tissues and normal liver tissue, resected away from the cancerous region, were obtained from patients, who underwent surgical excision of HCC at the Yangon Specialty Hospital (YSH), Myanmar. The tissue was fixed in 10% formalin at room temperature and embedded in paraffin using standard procedures. The samples used in this study were collected from 60 patients with HCC (age; 20–80 years, mean ± SD; 54.5 ± 11.2, 41 (67%) males and 19 (33%) females). Infection of hepatitis B virus (HBV) and hepatitis C virus (HCV) was tested with the rapid diagnostic test from Standard Diagnostics (Abbott Laboratories, Chicago, IL), Bioline HBsAg and Bioline HCV respectively.

This study was approved by the Ethics Review Committee of the Department of Medical Research, Yangon (#Ethics/DMR/2018/059), and informed consent was obtained from the patients in accordance with the Declaration of Helsinki. The clinical data of the patients are shown in the Table 1.

Histopathological examination

Paraffin embedded liver tissues, cut into 5 μm in thickness and placed onto the APS-coated slides, were stained with hematoxylin and eosin. The stained

Table 1. *Clinicopathological data of the 60 patients assessed in this study*

No.	Age	Sex	Histological Classification	HBV	HCV	Cyto c-Myc	Nuclear c-Myc	Cyto Pygo2	Nuclear Pygo2	PCNA	Cyto Bcl9
1	52	M	Normal	NA	NA	22.4	27.7	7.3	8.3	3.6	96.3
2	47	M	Normal	+	−	12.9	16.7	7.7	6.1	4.4	95.9
3	46	F	Normal	−	+	50.1	59.6	0.4	2.4	5.6	53.4
4	50	F	Normal	+	−	37.4	35.6	0.4	0.5	8.2	57.1
5	58	M	Normal	−	+	27.2	20.1	2.2	2.6	6.4	75.0
6	67	M	Well	−	+	13.9	28.3	17.6	37.9	24.8	59.9
7	71	M	Well	−	+	51.0	37.3	37.8	41.9	58.6	19.7
8	62	M	Well	−	+	37.5	39.5	14.5	27.6	27.6	32.3
9	57	M	Well	−	+	97.9	87.2	28.2	39.7	4.8	73.5
10	62	M	Well	+	−	97.9	83.2	34.5	49.6	15.0	15.5
11	60	M	Well	−	+	22.6	16.9	27.1	29.5	9.6	59.2
12	68	M	Well	+	−	65.2	80.0	24.5	50.8	32.6	13.5
13	43	M	Well	+	−	58.9	64.0	14.3	20.1	35.6	14.4
14	57	F	Well	−	+	16.9	26.2	13.3	25.8	37.2	34.4
15	80	M	Well	−	−	20.1	24.3	24.0	24.1	27.6	61.5
16	53	M	Well	−	+	41.1	48.9	17.8	19.9	37.8	11.9
17	54	F	Well	−	+	10.9	12.7	21.2	42.6	26.8	1.3
18	52	M	Well	+	−	13.7	18.9	22.3	31.1	21.8	18.7
19	64	M	Well	−	+	24.7	25.7	34.4	42.8	12.4	27.2
20	29	F	Well	−	−	28.6	23.2	18.8	32.1	9.6	2.6
21	54	M	Well	−	−	60.3	73.3	17.3	29.3	51.6	40.7
22	55	F	Well	+	−	56.7	45.8	3.4	17.9	12.4	57.9
23	46	M	Well	−	+	18.8	23.7	4.5	8.1	17.2	28.3
24	51	M	Well	NA	NA	52.5	56.0	15.0	35.0	14.8	37.8
25	37	M	Well	NA	NA	59.2	35.2	43.9	58.0	13.6	2.9
26	63	M	Moderate	−	+	2.1	6.7	21.9	21.4	48.8	1.7
27	53	F	Moderate	+	−	8.5	8.6	19.8	32.4	42.4	2.8
28	66	M	Moderate	−	+	48.6	41.0	1.1	16.0	5.0	2.7
29	59	F	Moderate	+	−	22.2	25.6	4.0	12.3	47.8	1.8
30	49	M	Moderate	+	−	9.2	19.6	11.6	21.6	24.0	3.9
31	63	F	Moderate	−	+	7.8	21.2	4.8	27.3	25.2	3.3
32	72	M	Moderate	+	−	9.1	14.0	19.6	35.8	24.2	8.2
33	63	F	Moderate	−	+	77.3	79.3	27.2	61.9	33.6	0.8
34	55	M	Moderate	+	−	28.5	20.9	10.9	24.5	18.4	6.0
35	51	M	Moderate	+	−	76.8	78.0	29.7	35.0	28.8	14.0
36	58	F	Moderate	−	+	30.7	39.5	22.1	43.7	62.4	2.9
37	60	M	Moderate	−	+	14.5	31.2	26.7	43.5	17.4	3.4
38	50	M	Moderate	−	+	19.6	32.5	27.5	59.4	67.2	1.6
39	66	M	Moderate	−	−	54.1	54.5	55.3	75.2	41.8	3.2
40	56	M	Moderate	+	−	62.6	64.9	13.1	16.2	30.8	4.9
41	77	F	Moderate	NA	NA	67.3	65.9	32.4	36.4	24.8	1.6
42	47	M	Moderate	−	+	87.4	73.7	32.4	39.8	5.6	9.4
43	53	F	Moderate	NA	NA	75.1	61.3	5.2	6.3	15.2	15.8
44	32	M	Moderate	NA	NA	48.7	44.7	22.3	19.2	45.2	0.1
45	39	M	Moderate	+	−	18.6	25.7	1.0	6.7	69.6	0.4
46	20	F	Moderate	+	−	48.9	61.8	4.3	3.4	25.0	0.3
47	39	M	Poor	+	−	39.2	38.3	17.7	58.3	73.6	0.0
48	40	M	Poor	+	−	56.0	52.4	28.5	51.3	62.4	0.2
49	61	M	Poor	+	−	85.2	101.0	31.9	48.3	48.0	2.4
50	62	F	Poor	−	+	99.2	102.2	7.0	36.4	36.6	1.2
51	64	F	Poor	−	−	81.5	98.1	37.5	65.7	65.0	0.1
52	61	M	Poor	+	−	61.9	71.3	16.4	48.9	56.2	10.8
53	54	F	Poor	−	+	43.2	56.6	14.5	44.8	41.6	1.5
54	51	M	Poor	−	+	105.9	117.5	39.7	74.3	72.6	11.8
55	55	F	Poor	−	+	85.6	92.8	14.4	71.7	77.0	2.4
56	43	M	Poor	+	+	57.6	55.4	27.8	47.1	18.8	1.8
57	58	M	Poor	−	+	50.3	97.8	25.3	50.3	57.4	0.2
58	62	F	Poor	+	−	68.5	62.3	14.5	22.8	25.4	3.0
59	42	M	Poor	+	−	56.9	55.0	10.4	17.3	37.2	0.4
60	51	M	Poor	+	+	51.1	47.4	24.7	50.6	57.2	2.7

HBV: Hepatitis B Virus; HCV: Hepatitis C Virus; M: Male; F: Female; NA: Not Available
+/−: Positive or Negative in HBV/HCV; PCNA: Proliferating Cell Nuclear Antigen

slides were examined histopathologically by two patholo-
gists who were blinded to the patients' data at Pathology
Research Division, Department of Medical Research
(DMR), Yangon. Tissue samples were assessed using the
WHO classification. Out of the 60 examined cases, 5 cases
(8%) were considered normal and 55 (92%) were diag-
nosed as HCC. Regarding the histopathological grade, 20
cases were graded as well differentiated, 21 cases as mod-
erately differentiated and 14 cases as poorly differentiated
HCC. The results of histopathological examination are
summarized in Table 1.

Immunohistochemistry

All procedures were performed according to the
methods reported previously [35, 47]. Briefly, paraffin-
embedded tissues were serially cut into 5-μm-thick sections
and placed onto APS-coated glass slides. After deparaf-
finization and rehydration followed by autoclaving in
10 mM citrate buffer (pH 6.0, 120°C, 15 min), endoge-
nous peroxidase activity was inactivated with 0.3% H_2O_2/
methanol for 15 min. The specimens were incubated with
normal goat IgG (500 μg/ml) and bovine serum albumin
(1%, BSA) in phosphate buffered saline (PBS) for 1 hr to
block non-specific binding of antibodies and then incubated
overnight with the primary antibody in 1% BSA/PBS.
After triplicate washing with 0.075% Brij/PBS for 10 min
each, the specimens were reacted with HRP-conjugated
secondary antibodies for 1 hr. After 3 times washing with
0.075% Brij/PBS, the signal was visualized with DAB and
H_2O_2 in the presence of nickel and cobalt ions [10, 49].
In each experimental run, normal mouse IgG was applied
as a negative control at the same concentration instead of
the specific primary antibody. Finally, the specimens were
mounted with Permount after dehydration through ethanol-
xylene series.

In situ hybridization

The sequence of nucleotide no. 489 to 525 of human
(h) Pygo2 (CTTGGCAGTCCTGTGCCCTTCGGAGGCTT
CCGTGTGC) was used as the sense hPygo2 probe and
complementary to this sequence was used as an antisense
hPygo2 probe (GCACACGGAAGCCTCCGAAGGGCAC
AGGACTGCCAAG). Furthermore, a 28S rRNA probe was
used to estimate the level of hybridizable RNAs in the tis-
sue sections [57]. The antisense sequence of 28s rRNA was
(TGCTACTACCACCAAGATCTGCACCTGCGGCGGC).
These probes were labeled by digoxigenin according to
the protocol described in our previous study [27]. The
specificity and sensitivity of the oligo-DNA probes were
confirmed by immunodetection and dot blot hybridization.
The procedure of *in situ* hybridization was performed as
described in detail previously [28, 55]. After deparaffiniza-
tion and rehydration, the sections were treated with 0.2 N
hydrochloric acid for 20 min and digested with 50 μg/ml of
proteinase K for 15 min at 37°C. After post-fixation with
4% paraformaldehyde in PBS for 5 min, the sections were

immersed in 2 mg/ml glycine in PBS for 15 min twice and
kept in 40% deionized formamide in 4 × standard saline
citrate (SSC; 1 × SSC = 0.15 M sodium chloride and 0.015
M sodium citrate, pH 7.0) until used for hybridization.
Hybridization was carried out for 15–17 hr at 37°C with
2 μg/ml hPygo2 DIG-labeled probe in the hybridization
medium containing 10 mM Tris/HCl, 0.6 M NaCl, 1 mM
EDTA, 1× Denhardt's solution, 250 μg/ml of yeast tRNA,
125 μg/ml of salmon testes DNA, 10% dextran sulfate
in deionized formamide solution. After hybridization, the
slides were washed 4 times with 40% formamide/2 × SSC
for 1 hr each wash at 37°C, and followed by 2 × SSC at
room temperature (RT). Then, the sections were reacted
with the blocking solution (100 μg/ml of yeast tRNA, 100
μg/ml of salmon sperm DNA and 500 μg/ml of normal goat
IgG in 5% BSA/PBS solution) for 1 hr, reacted overnight
with horseradish peroxidase (HRP)-conjugated goat anti-
digoxigenin antibody (Roche) in blocking solution, and
washed four times with 0.075% Brij/PBS for 15 min each.
The signals were visualized with 3,3'-diaminobenzidine
(DAB) and H_2O_2 with nickel and cobalt ions, as described
previously [27]. Unless otherwise specified, all procedures
were performed at RT.

Quantitative analysis

Three randomly selected areas in each specimen were
photographed at 400× magnification and each 8-bit image
was then assessed with ImageJ or Fiji software. The aver-
age of pixels/dot (1 to 255) of the cytoplasm or nucleus
was obtained by surrounding the region of interest with
the ROI manager. The total pixel/dot of the cytoplasm and
nuclei for the image was counted using more than 100 cells
(>30 cells/area). The reported immunohistochemistry signal
intensity represented the positive subtracting from the latter
the average pixels/dot of the negative control. PCNA label-
ing index represented the percentage of cells with positive
nuclei per total number of counted nuclei.

Statistical analysis

One-way ANOVA followed by Tukey's range test was
used to compare the signal intensity between the normal
liver tissue and each histopathological grade of HCC. A
P value < 0.05 denoted the presence of a statistically
significant difference. The Wilcoxon-Mann-Whitney test
was performed to compare between two groups. All statis-
tical analyses were conducted using the KaleidaGraph 4
(Hulinks Inc., Tokyo), except for Spearman's correlation
rank test, which was performed using Microsoft Excel
(Office 365, Microsoft Corp.).

III. Results

Cytoplasmic and nuclear Pygo2 and Bcl9 expression profiles in Myanmar HCC

Immunohistochemistry was used to map Pygo2 sites
in normal liver tissue and various histopathological grades

of HCC using an antibody against human Pygo2. Staining for Pygo2 was not detected in the normal liver tissue but positive in both the cytoplasm and nuclei of cancer cells and the density of staining increased with advances in histopathological grade of HCC (Fig. 1a). The nuclear staining of Pygo2 was especially strong in poorly differentiated HCC. The signal intensity of both cytoplasmic and nuclear Pygo2 was significantly higher in HCC than in normal (Fig. 1b and c). The median intensity of cytoplasmic Pygo2 in normal and HCC was 2.2 and 19.8, respectively, whereas those in nuclear Pygo2 in normal and HCC was 2.6 and 35.8, respectively. The signal intensity of Pygo2 in 51 out of 55 HCC cases (93%) was larger than the highest (8.29) in normal liver tissue (Table 1). The signal intensity of cytoplasmic Pygo2 did not show significant difference among the histopathological grade of HCC (Fig. 1d), while the nuclear signal was significantly higher in poorly differentiated HCC than well and moderately differentiated one (Fig. 1e).

The expression of Bcl9 was examined in sections adjacent to those used for assessment of Pygo2 expression with the antibody that specifically recognize cytoplasmic but not nuclear Bcl9 (Fig. 1a). With this antibody, we previously revealed that the loss of cytoplasmic Bcl9 was associated with the progression of histopathological grade of HCC in Myanmar [41]. In agreement with that findings, cytoplasmic Bcl9 expression was noted in the normal liver tissue, but was decreased in well differentiated HCC and almost negative in moderately and poorly differentiated HCC. Statistical analysis indicated significantly weak signal intensity of Bcl9 in all HCC compared to normal, and was barely positive in moderately and poorly differentiated HCC (Fig. 1f).

In situ detection of Pygo2 mRNA in Myanmar HCC

The above results of Pygo2 immunohistochemistry indicated upregulation of Pygo2 in HCC, especially in poorly differentiated tumors. Accordingly, we examined next the signal intensity of Pygo2 mRNA by *in situ* hybridization to confirm the transcriptional activation of Pygo2. For accurate comparison among the cases, we had preliminarily selected five cases each from normal and various histopathological grades of HCC, those retained well-preserved RNA assessed by *in situ* hybridization of 28S rRNA [57]. Figure 2a shows the average signal intensity obtained by *in situ* hybridization using Pygo2 sense and antisense, and 28S rRNA probes. There was no significant difference in 28S rRNA retention among the cases. The expression of Pygo2 mRNA was detected in the cytoplasm of all HCC differentiation grades but not in normal liver tissue (Fig. 2b). Statistical analysis indicated significant Pygo2 expression in HCC compared to normal liver tissue, and that the expression was not influenced by histopathological grading (Fig. 2c).

Cytoplasmic and nuclear Myc and PCNA expression profiles in Myanmar HCC

Selecting tissue sections adjacent to those used for Pygo2 immunohistochemistry, we conducted immunohistochemistry of Myc (Fig. 3a). Myc was expressed in the cytoplasm and nuclei of hepatocytes found in the normal liver tissue as well as in the cancer cells of all HCC, although the expression was weakest in the normal liver tissue relative to the cancerous areas. Analysis of the immunostaining pattern according to the histopathological grade showed the strongest staining in the cytoplasm and nuclei of poorly differentiated HCC. Furthermore, the signal intensities of the cytoplasmic and nuclear Myc were significantly higher in poorly differentiated HCC compared to the normal, as well as the well and moderately differentiated HCC (Fig. 3b and c).

We also immunohistochemically stained serial sections adjacent to those used for Myc immunohistochemistry for PCNA. PCNA was increased progressively with the progression of histopathological grade (Fig. 3a). Statistical analysis revealed that the PCNA labeling index was significantly higher in poorly differentiated HCC than normal liver tissue, as well as in well and moderately differentiated HCC, while the staining in moderately differentiated HCC was also significantly higher than the normal liver tissue (Fig. 3d).

Correlation analysis of Pygo2, Bcl9, Myc, and PCNA immunohistochemical staining

Comparison of the distribution of Pygo2, Bcl9, Myc, and PCNA signals in serial sections revealed co-localization of Pygo2, Myc and PCNA in the same tumor nest and partially in the same individual tumor cells (Fig. 1a). This finding suggests potential correlation in the expression of these molecules in Myanmar HCC. Accordingly, this was tested in the next step of the study.

The signal intensity of nuclear Pygo2 correlated significantly with those of nuclear Myc (Fig. 4c, R = 0.39, $P < 0.01$), PCNA (Fig. 4d, R = 0.46, $P < 0.001$), as well as cytoplasmic Pygo2 (Fig. 4e, R = 0.78, $P < 0.001$), and inversely with that of cytoplasmic Bcl9 (Fig. 4b, R = −0.36, $P < 0.01$). Furthermore, the signal intensity of nuclear Myc also correlated significantly with that of PCNA (Fig. 4f, R = 0.26, $P < 0.05$), whereas that of cytoplasmic Bcl9 correlated inversely with PCNA (Fig. 4g, R = −0.59, $P < 0.001$) but not with nuclear Myc.

Possible correlation between signal intensity and the clinicopathological features

Finally, we analyzed the correlation of cytoplasmic/nuclear Pygo2, cytoplasmic Bcl9, cytoplasmic/nuclear Myc and PCNA with the clinicopathological features of HCC. Cytoplasmic Bcl9 correlated with the development of HCC in younger patients (<40 years and >40 years, $P = 0.0007$) as was reported previously [20], while Pygo2 did not ($P = 1.00$) probably because of its low expression in 2 out
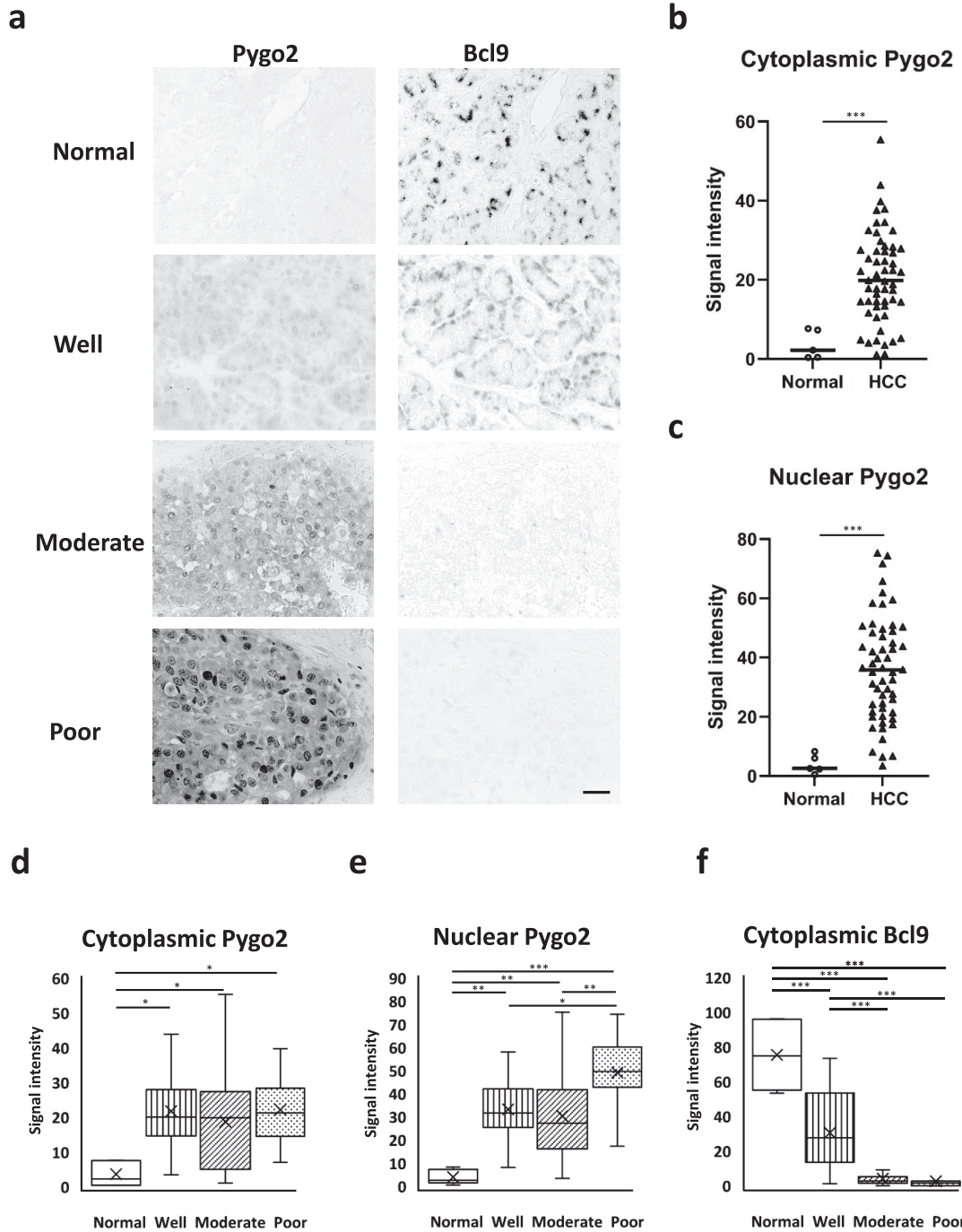
Fig. 1. Immunohistochemistry of Pygo2 and Bcl9 in serial sections of Myanmar HCC and comparison of the signal intensity. (**a**) Immunohistochemistry of Pygo2 (left column) and Bcl9 (right column) in serial sections of normal liver tissue, well, moderately and poorly differentiated HCC. Bar = 100 μm. Comparison of the signal intensity of cytoplasmic Pygo2 (**b**), nuclear Pygo2 (**c**) between normal areas and HCC. The bar indicated the median intensity of cytoplasmic and nuclear Pygo2 in normal and HCC. Comparison of the signal intensity of cytoplasmic Pygo2 (**d**), nuclear Pygo2 (**e**) and cytoplasmic Bcl9 (**f**) among normal liver tissue, well, moderately and poorly differentiated HCC using box and whisker plots. *$P < 0.05$, **$P < 0.01$ and ***$P < 0.001$.

of 7 patients who developed HCC at young age (Table 1, Cases #45 and #46). Pygo2 did not correlate with sex ($P = 0.44$), HBV ($P = 0.19$) or HCV infection ($P = 0.22$). More-over, Myc and PCNA expression level did not correlate with any of the clinicopathological parameters examined in this study.

a

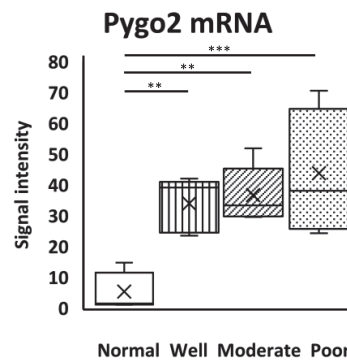|	Normal	Well	Moderate	Poor
Pygo2 (anti-sense) (Mean ± SD)	65.5±6.1	86.2±11.9	99.5±13.9	96.1±10.4
Pygo2 (sense) (Mean ± SD)	60.2±2.5	52.2±11.5	62.8±20.5	52.3±19.1
28s rRNA (Mean ± SD)	149.3±9.1	142.8±4.8	138.0±8.9	149.7±11.0

b
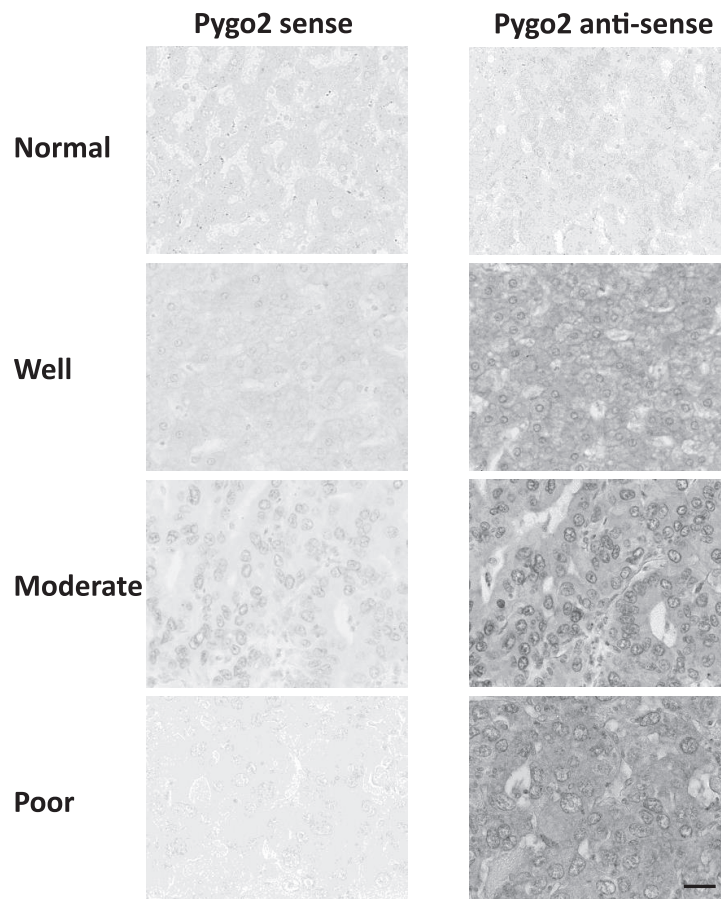
c

Fig. 2. *In situ* hybridization for detection of Pygo2 mRNA and comparison of the signal intensity. (**a**) Signal intensity detected with sense and antisense hPygo2 probes, and 28s rRNA probes. Data are mean ± SD. (**b**) *In situ* hybridization using sense (left column) and antisense (right column) probes of hPygo2 in normal liver tissue, well, moderately and poorly differentiated HCC. Bar = 100 μm. (**c**) Comparison of signal intensity of Pygo2 mRNA among normal liver tissue, well, moderately and poorly differentiated HCC using box and whisker plots. The mRNA level of Pygo2 in each sample was obtained by subtracting the value of sense from antisense. **$P < 0.01$ and ***$P < 0.001$.
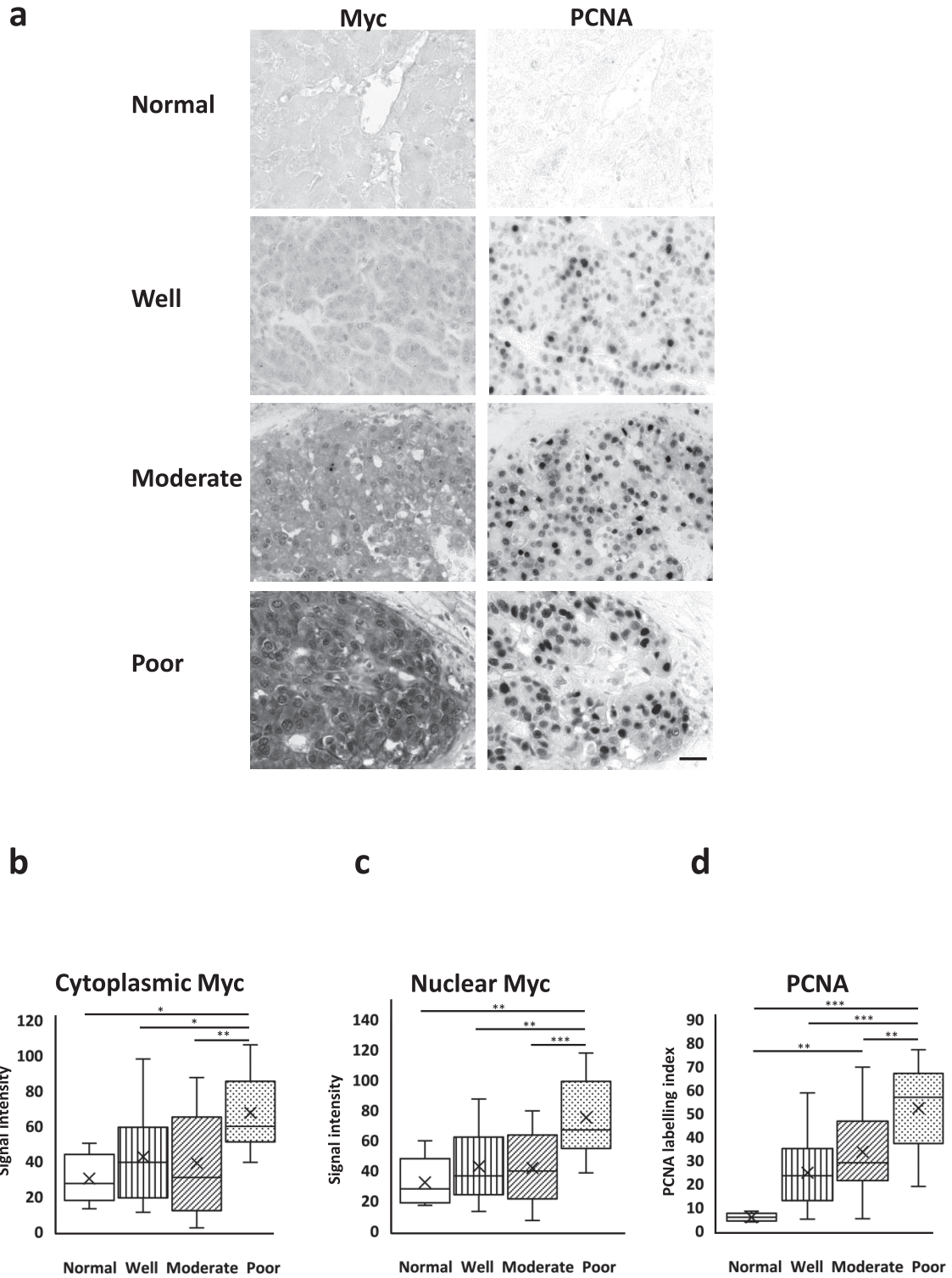
Fig. 3. Immunohistochemistry of Myc and PCNA in Myanmar HCC and comparison of the signal intensity. (**a**) Immunohistochemistry of Myc (left column) and PCNA (right column) of serial sections of normal liver tissue, well, moderately and poorly differentiated HCC obtained from the sections adjacent to those used in Fig. 1a. Bar = 100 μm. Comparison of the signal intensity of cytoplasmic Myc (**b**), nuclear Myc (**c**) and PCNA labelling index (**d**) among normal liver tissue, well, moderately and poorly differentiated HCC using box and whisker plots. *$P < 0.05$, **$P < 0.01$ and ***$P < 0.001$. Images in this figure are from sections adjacent to those of Fig. 1.

a

	Nuclear Pygo2	Cytoplasmic Bcl9	Nuclear Myc	PCNA	Cytoplasmic Pygo2	Cytoplasmic Myc
Nuclear Pygo2	1					
Cytoplasmic Bcl9	R = -0.3643 (P = 0.00421)	1				
Nuclear Myc	R = 0.3885 (P = 0.00216)	R = -0.1968 (P = 0.13171)	1			
PCNA	R = 0.4643 (P = 0.00019)	R = -0.5854 (P = 9E-07)	R = 0.2585 (P = 0.04609)	1		
Cytoplasmic Pygo2	R = 0.7757 (P = 3.40209E-13)	R = -0.1672 (P = 0.20152)	R = 0.2663 (P = 0.03972)	R = 0.2433 (P = 0.06106)	1	
Cytoplasmic Myc	R = 0.3677 (P = 0.00385)	R = -0.1255 (P = 0.33942)	R = 0.9231 (P = 9.4E-26)	R = 0.1277 (P = 0.33072)	R= 0.3247 (P = 0.01137)	1
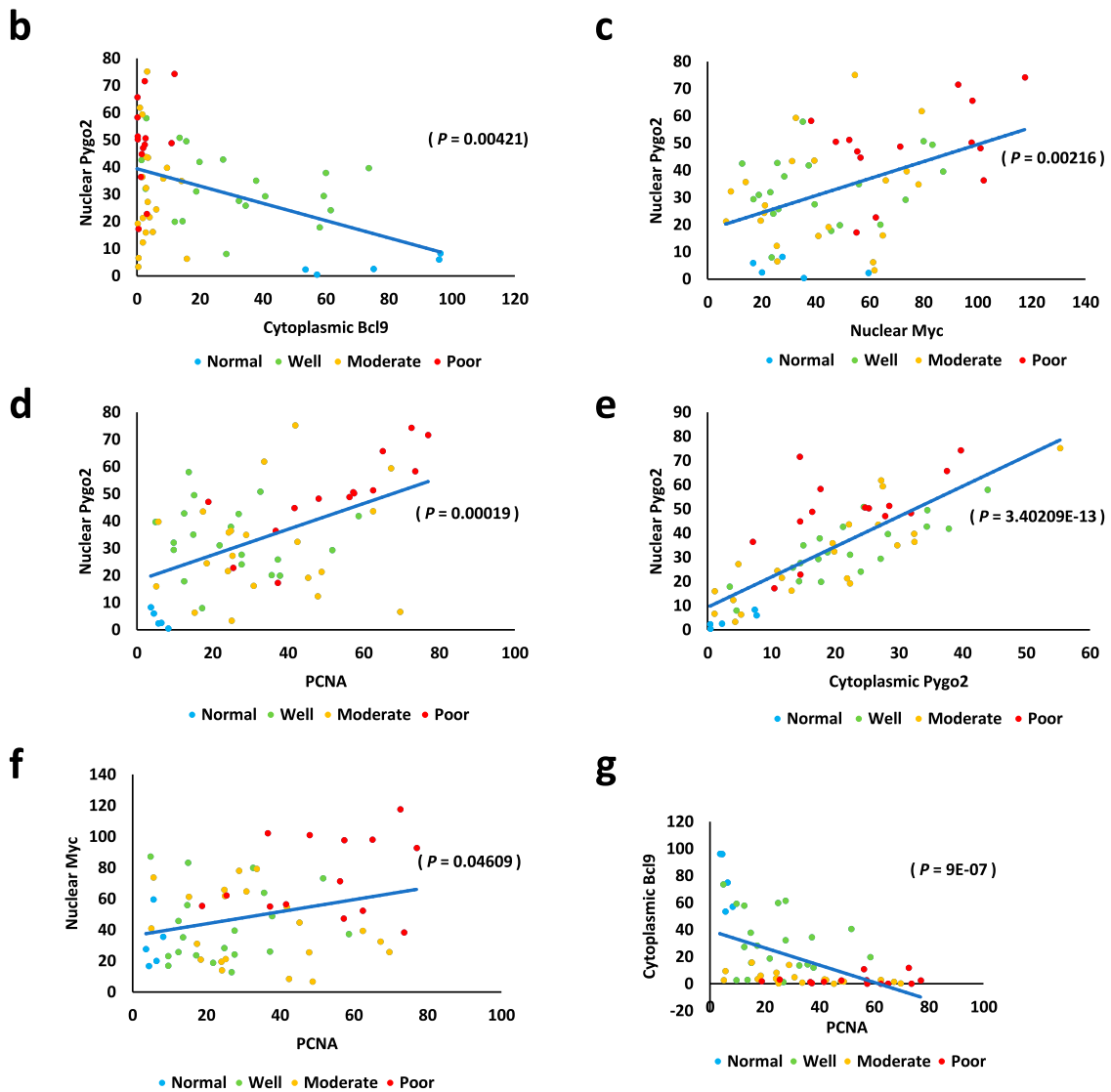
Fig. 4. Correlation analysis of the signal intensities of Pygo2, Bcl9, Myc and PCNA in Myanmar HCC. (**a**) Results of Spearman's correlation rank test. (**b–g**) Scatter plot of Pygo2 and cytoplasmic Bcl9 (**b**), nuclear Pygo2 and nuclear Myc (**c**), nuclear Pygo2 and PCNA (**d**), nuclear Pygo2 and cytoplasmic Pygo2 (**e**), nuclear Myc and PCNA (**f**) and, cytoplasmic Bcl9 and PCNA (**g**). The P value in each graph was calculated by Spearman's correlation rank test.

IV. Discussion

In the present study, we revealed the expression of nuclear Pygo2 in more than 90% of Myanmar HCC cases, with the strongest expression in poorly differentiated HCC. Furthermore, nuclear Pygo2 expression correlated with loss of cytoplasmic Bcl9, nuclear Myc and PCNA labeling index. These results suggest common activation of both Wnt/β-catenin and Myc signaling in Myanmar HCC and that the correlated activation profiles of Pygo2 and Myc could characterize the malignant state of HCC in Myanmar.

Previous studies reported abnormal upregulation of Pygo2 in HCC and that its aberrant nuclear localization correlated with age, tumor size, metastasis, vascular invasion and tumor differentiation [39, 58]. Moreover, it was reported that Bcl9 was overexpressed in HCC and its nuclear localization correlated with microvascular invasion, metastasis and poor prognosis [18, 19]. These reports seem to be consistent with the function of Pygo2 and Bcl9 as co-activators in Wnt/β-catenin signaling. Until now, however, neither simultaneous distribution of Pygo2 and Bcl9 nor their correlation has not been reported in HCC, probably because both Pygo2 and Bcl9 have their own functions independent of Wnt/β-catenin signaling, such as Pygo2 effect on eye and testis development and the regulation of enamel production by Bcl9 [7, 8, 9, 42]. Our findings seem to provide evidence that Pygo2 and Bcl9 act together as co-activators of Wnt/β-catenin signaling in Myanmar HCC. In this context, it should be noted that unexpectedly low levels of both nuclear Pygo2 and cytoplasmic Bcl9 were found in our study in a few HCC young patients. In these cases, Bcl9 might exert its special function independent of Wnt/β-catenin signaling, which is essential in the development or progression of HCC in these particular cases.

Previous study reported that 66.7% of their cases with HCC expressed nuclear Pygo2 [58], whereas Xu *et al.* reported 34.4% of HCC expressed Bcl9 [54]. Nuclear accumulation of β-catenin was reported in 40 to 70% of HCC patients [16, 24, 31, 36]. In Japanese, Midorikawa *et al.* [33] reported that nuclear localization of β-catenin was limited in overt HCC but not in the early stage of HCC. Based on this background, Wnt/β-catenin signaling seems to be constantly activated in Myanmar HCC, since Pygo2 nuclear accumulation was detected in over 90% of the cases in Myanmar HCC. The frequent activation of the signaling could be a potentially useful marker for Myanmar HCC, although the same experiment should be performed in the cases of the other countries. While our study did not directly address the mechanism that activate Wnt/β-catenin signaling in Myanmar HCC, previous studies demonstrated that iron chelators can modulate Wnt/β-catenin signaling *in vitro* [13, 21, 53]. Excess iron uptake in Myanmar could be potentially the reason for the upregulation of the signaling, as reported previously [2, 40]. Further *in vitro* studies for exploring the relevance between Pygo2 and iron is needed.

Frequent Myc amplification is reported in young HCC patients and those with poor prognosis [20, 44]. Amplification of Myc genes is the major genetic alteration and leads to deregulation of Myc genes in human tumors, while aberrant Myc expression can also be caused by defects in any of the upstream signaling pathways [32]. Myc is one of the transcriptional targets of Wnt/β-catenin signaling, while the epistatic relationship has not been recognized in mouse liver, different from colon cancer [45]; Myc was not expressed in hyperplastic liver and well differentiated liver tumor in APC-loss-of-function (LOF) mouse [12, 22], and Myc deletion failed to suppress hepatocyte proliferation induced by APC-LOF [37]. Since our study showed no significant cytoplasmic correlation between Bcl9 and Myc, it is likely that upregulation of Myc is not directly controlled by the Wnt/β-catenin signaling in Myanmar HCC. Pygo2, however, is reported to play Wnt/β-catenin independent role in lens and testis development and tumor progression [8, 42, 50]. One should not rule out the possibility that Pygo2 regulates Myc expression independent of β-catenin [3], in addition to other upstream signaling, such as Notch, Sonic hedgehog, MAPK pathways [17, 26, 43, 52], or recurrent secondary genetic rearrangements [22].

Accumulating evidence suggests that co-activation of the Wnt/β-catenin and Myc signaling correlates with poor prognosis of HCC [4, 12, 22, 37]. In agreement with these report, our study revealed that progression of histopathological grade of Myanmar HCC correlated with intense nuclear Pygo2 immunostaining, nuclear Myc expression and high PCNA index. Our results suggest that the expression profiles of both Pygo2 and Myc are potentially suitable markers for prognosis of Myanmar HCC. Given that Pygo2 regulates the expression of Myc target gene [3], we consider that Pygo2 is also a suitable therapeutic target for the design of new therapies that do not only diminish the activity of Wnt/β-catenin signaling but also reduce the activation of Myc-target genes in Myanmar HCC.

V. Conflicts of Interest

The authors declare no conflict of interest.

VI. Acknowledgments

VII. References

1. Allen-Petersen, B. L. and Sears, R. C. (2019) Mission Possible: Advances in MYC Therapeutic Targeting in Cancer. *BioDrugs* 33; 539–553.
2. An, S., Soe, K., Akamatsu, M., Hishikawa, Y. and Koji, T.

(2012) Accelerated proliferation of hepatocytes in rats with iron overload after partial hepatectomy. *Histochem. Cell Biol.* 138; 773–786.

3. Andrews, P. G. P., Popadiuk, C., Belbin, T. J. and Kao, K. R. (2018) Augmentation of Myc-Dependent Mitotic Gene Expression by the Pygopus2 Chromatin Effector. *Cell Rep.* 23; 1516–1529.

4. Bisso, A., Filipuzzi, M., Gamarra Figueroa, G. P., Brumana, G., Biagioni, F., Doni, M., *et al.* (2020) Cooperation Between MYC and β-Catenin in Liver Tumorigenesis Requires Yap/Taz. *Hepatology* 72; 1430–1443.

5. Bosch, F. X., Ribes, J., Díaz, M. and Cléries, R. (2004) Primary liver cancer: worldwide incidence and trends. *Gastroenterology* 127; S5–S16.

6. Calvisi, D. F., Factor, V. M., Loi, R. and Thorgeirsson, S. S. (2001) Activation of beta-catenin during hepatocarcinogenesis in transgenic mouse models: relationship to phenotype and tumor grade. *Cancer Res.* 61; 2085–2091.

7. Cantù, C., Pagella, P., Shajiei, T. D., Zimmerli, D., Valenta, T., Hausmann, G., *et al.* (2017) A cytoplasmic role of Wnt/β-catenin transcriptional cofactors Bcl9, Bcl9l, and Pygopus in tooth enamel formation. *Sci. Signal.* 10; eaah4598.

8. Cantù, C., Valenta, T., Hausmann, G., Vilain, N., Aguet, M. and Basler, K. (2013) The Pygo2-H3K4me2/3 interaction is dispensable for mouse development and Wnt signaling-dependent transcription. *Development* 140; 2377–2386.

9. Cantù, C., Zimmerli, D., Hausmann, G., Valenta, T., Moor, A., Aguet, M., *et al.* (2014) Pax6-dependent, but β-catenin-independent, function of Bcl9 proteins in mouse lens development. *Genes Dev.* 28; 1879–1884.

10. Choijookhuu, N., Sato, Y., Nishino, T., Endo, D., Hishikawa, Y. and Koji, T. (2012) Estrogen-dependent regulation of sodium/hydrogen exchanger-3 (NHE3) expression via estrogen receptor β in proximal colon of pregnant mice. *Histochem. Cell Biol.* 137; 575–587.

11. Clevers, H. (2006) Wnt/beta-catenin signaling in development and disease. *Cell* 127; 469–480.

12. Colnot, S., Decaens, T., Niwa-Kawakita, M., Godard, C., Hamard, G., Kahn, A., *et al.* (2004) Liver-targeted disruption of Apc in mice activates beta-catenin signaling and leads to hepatocellular carcinomas. *Proc. Natl. Acad. Sci. U S A* 101; 17216–17221.

13. Coombs, G. S., Schmitt, A. A., Canning, C. A., Alok, A., Low, I. C., Banerjee, N., *et al.* (2012) Modulation of Wnt/β-catenin signaling and proliferation by a ferrous iron chelator with therapeutic efficacy in genetically engineered mouse models of cancer. *Oncogene* 31; 213–225.

14. de La Coste, A., Romagnolo, B., Billuart, P., Renard, C. A., Buendia, M. A., Soubrane, O., *et al.* (1998) Somatic mutations of the beta-catenin gene are frequent in mouse and human hepatocellular carcinomas. *Proc. Natl. Acad. Sci. U S A* 95; 8847–8851.

15. Gao, W., Kim, H., Feng, M., Phung, Y., Xavier, C. P., Rubin, J. S., *et al.* (2014) Inactivation of Wnt signaling by a human antibody that recognizes the heparan sulfate chains of glypican-3 for liver cancer therapy. *Hepatology* 60; 576–587.

16. Guo, Y., Zhao, Y. R., Liu, H., Xin, Y., Yu, J. Z., Zang, Y. J., *et al.* (2021) EHMT2 promotes the pathogenesis of hepatocellular carcinoma by epigenetically silencing APC expression. *Cell Biosci.* 11; 152.

17. He, T. C., Sparks, A. B., Rago, C., Hermeking, H., Zawel, L., da Costa, L. T., *et al.* (1998) Identification of c-MYC as a target of the APC pathway. *Science* 281; 1509–1512.

18. Huge, N., Sandbothe, M., Schröder, A. K., Stalke, A., Eilers, M., Schäffer, V., *et al.* (2020) Wnt status-dependent oncogenic role of BCL9 and BCL9L in hepatocellular carcinoma. *Hepatol. Int.* 14; 373–384.

19. Hyeon, J., Ahn, S., Lee, J. J., Song, D. H. and Park, C. K. (2013) Prognostic Significance of BCL9 Expression in Hepatocellular Carcinoma. *Korean J. Pathol.* 47; 130–136.

20. Jaskiewicz, K. and Banach, L. (1996) Hepatocellular carcinoma in young patients. *Oncol. Rep.* 3; 1187–1189.

21. Kamihara, Y., Takada, K., Sato, T., Kawano, Y., Murase, K., Arihara, Y., *et al.* (2016) The iron chelator deferasirox induces apoptosis by targeting oncogenic Pyk2/β-catenin signaling in human multiple myeloma. *Oncotarget* 7; 64330–64341.

22. Kaveri, D., Kastner, P., Dembélé, D., Nerlov, C., Chan, S. and Kirstetter, P. (2013) β-Catenin activation synergizes with Pten loss and Myc overexpression in Notch-independent T-ALL. *Blood* 122; 694–704.

23. Kew, M. C. (2010) Epidemiology of chronic hepatitis B virus infection, hepatocellular carcinoma, and hepatitis B virus-induced hepatocellular carcinoma. *Pathol. Biol. (Paris)* 58; 273–277.

24. Kim, E., Lisby, A., Ma, C., Lo, N., Ehmer, U., Hayer, K. E., *et al.* (2019) Promotion of growth factor signaling as a critical function of β-catenin during HCC progression. *Nat. Commun.* 10; 1909.

25. Klaus, A. and Birchmeier, W. (2008) Wnt signalling and its impact on development and cancer. *Nat. Rev. Cancer* 8; 387–398.

26. Knoepfler, P. S. and Kenney, A. M. (2006) Neural precursor cycling at sonic speed: N-Myc pedals, GSK-3 brakes. *Cell Cycle* 5; 47–52.

27. Koji, T. and Brenner, R. M. (1993) Localization of estrogen receptor messenger ribonucleic acid in rhesus monkey uterus by nonradioactive in situ hybridization with digoxigenin-labeled oligodeoxynucleotides. *Endocrinology* 132; 382–392.

28. Koji, T. and Nakane, P. K. (1996) Recent advances in molecular histochemical techniques: in situ hybridization and southwestern histochemistry. *J. Electron. Microsc. (Tokyo)* 45; 119–127.

29. Kramps, T., Peter, O., Brunner, E., Nellen, D., Froesch, B., Chatterjee, S., *et al.* (2002) Wnt/wingless signaling requires BCL9/legless-mediated recruitment of pygopus to the nuclear beta-catenin-TCF complex. *Cell* 109; 47–60.

30. Krutsenko, Y., Singhi, A. D. and Monga, S. P. (2021) β-Catenin Activation in Hepatocellular Cancer: Implications in Biology and Therapy. *Cancers (Basel)* 13; 1830.

31. Lachenmayer, A., Alsinet, C., Savic, R., Cabellos, L., Toffanin, S., Hoshida, Y., *et al.* (2012) Wnt-pathway activation in two molecular classes of hepatocellular carcinoma and experimental modulation by sorafenib. *Clin. Cancer Res.* 18; 4997–5007.

32. Lin, C. Y., Lovén, J., Rahl, P. B., Paranal, R. M., Burge, C. B., Bradner, J. E., *et al.* (2012) Transcriptional amplification in tumor cells with elevated c-Myc. *Cell* 151; 56–67.

33. Midorikawa, Y., Yamamoto, S., Tatsuno, K., Renard-Guillet, C., Tsuji, S., Hayashi, A., *et al.* (2020) Accumulation of Molecular Aberrations Distinctive to Hepatocellular Carcinoma Progression. *Cancer Res.* 80; 3810–3819.

34. Miyoshi, Y., Iwao, K., Nagasawa, Y., Aihara, T., Sasaki, Y., Imaoka, S., *et al.* (1998) Activation of the beta-catenin gene in primary hepatocellular carcinomas by somatic alterations involving exon 3. *Cancer Res.* 58; 2524–2527.

35. Nakajima, K., Shibata, Y., Hishikawa, Y., Suematsu, T., Mori, M., Fukuhara, S., *et al.* (2014) Coexpression of ang1 and tie2 in odontoblasts of mouse developing and mature teeth-a new insight into dentinogenesis. *Acta Histochem. Cytochem.* 47; 19–25.

36. Pez, F., Lopez, A., Kim, M., Wands, J. R., Caron de Fromentel, C. and Merle, P. (2013) Wnt signaling and hepatocarcinogenesis: molecular targets for the development of innovative anticancer

drugs. *J. Hepatol.* 59; 1107–1117.

37. Reed, K. R., Athineos, D., Meniel, V. S., Wilkins, J. A., Ridgway, R. A., Burke, Z. D., *et al.* (2008) B-catenin deficiency, but not Myc deletion, suppresses the immediate phenotypes of APC loss in the liver. *Proc. Natl. Acad. Sci. U S A* 105; 18919–18923.

38. Saxena, M., Kalathur, R. K. R., Rubinstein, N., Vettiger, A., Sugiyama, N., Neutzner, M., *et al.* (2020) A Pygopus 2-Histone Interaction Is Critical for Cancer Cell Dedifferentiation and Progression in Malignant Breast Cancer. *Cancer Res.* 80; 3631–3648.

39. Skawran, B., Steinemann, D., Weigmann, A., Flemming, P., Becker, T., Flik, J., *et al.* (2008) Gene expression profiling in hepatocellular carcinoma: upregulation of genes in amplified chromosome regions. *Mod. Pathol.* 21; 505–516.

40. Soe, K., Hishikawa, Y., Fukuzawa, Y., Win, N., Yin, K. S., Win, K. M., *et al.* (2007) Possible correlation between iron deposition and enhanced proliferating activity in hepatitis C virus-positive hepatocellular carcinoma in Myanmar (Burma). *J. Gastroenterol.* 42; 225–235.

41. Soe, M. T., Shibata, Y., Win Htun, M., Abe, K., Soe, K., Win Than, N., *et al.* (2019) Immunohistochemical Mapping of Bcl9 Using Two Antibodies that Recognize Different Epitopes Is Useful to Characterize Juvenile Development of Hepatocellular Carcinoma in Myanmar. *Acta Histochem. Cytochem.* 52; 9–17.

42. Song, N., Schwab, K. R., Patterson, L. T., Yamaguchi, T., Lin, X., Potter, S. S., *et al.* (2007) pygopus 2 has a crucial, Wnt pathway-independent function in lens induction. *Development* 134; 1873–1885.

43. Stefan, E. and Bister, K. (2017) MYC and RAF: Key Effectors in Cellular Signaling and Major Drivers in Human Cancer. *Curr. Top. Microbiol. Immunol.* 407; 117–151.

44. Takahashi, Y., Kawate, S., Watanabe, M., Fukushima, J., Mori, S. and Fukusato, T. (2007) Amplification of c-myc and cyclin D1 genes in primary and metastatic carcinomas of the liver. *Pathol. Int.* 57; 437–442.

45. Talla, S. B. and Brembeck, F. H. (2016) The role of Pygo2 for Wnt/ß-catenin signaling activity during intestinal tumor initiation and progression. *Oncotarget* 7; 80612–80632.

46. Tetsu, O. and McCormick, F. (1999) Beta-catenin regulates expression of cyclin D1 in colon carcinoma cells. *Nature* 398; 422–426.

47. Tun, N., Shibata, Y., Soe, M. T., Htun, M. W. and Koji, T. (2019) Histone deacetylase inhibitors suppress transdifferentiation of gonadotrophs to prolactin cells and proliferation of prolactin cells induced by diethylstilbestrol in male mouse pituitary. *Histochem. Cell Biol.* 151; 291–303.

48. Turlin, B., Juguet, F., Moirand, R., Le Quilleuc, D., Loréal, O., Campion, J. P., *et al.* (1995) Increased liver iron stores in patients with hepatocellular carcinoma developed on a noncirrhotic liver.

Hepatology 22; 446–450.

49. Ulziibat, S., Ejima, K., Shibata, Y., Hishikawa, Y., Kitajima, M., Fujishita, A., *et al.* (2006) Identification of estrogen receptor beta-positive intraepithelial lymphocytes and their possible roles in normal and tubal pregnancy oviducts. *Hum. Reprod.* 21; 2281–2289.

50. Vafaizadeh, V., Buechel, D., Rubinstein, N., Kalathur, R. K. R., Bazzani, L., Saxena, M., *et al.* (2021) The interactions of Bcl9/Bcl9L with beta-catenin and Pygopus promote breast cancer growth, invasion, and metastasis. *Oncogene* 40; 6195–6209.

51. Wang, W., Smits, R., Hao, H. and He, C. (2019) Wnt/β-Catenin Signaling in Liver Cancers. *Cancers (Basel)* 11; 926.

52. Weng, A. P., Millholland, J. M., Yashiro-Ohtani, Y., Arcangeli, M. L., Lau, A., Wai, C., *et al.* (2006) c-Myc is an important direct target of Notch1 in T-cell acute lymphoblastic leukemia/lymphoma. *Genes Dev.* 20; 2096–2109.

53. Xu, W., Yu, R., Zhu, X., Li, Z., Jia, J., Li, D., *et al.* (2020) Iron-Chelating Agent Can Maintain Bone Homeostasis Disrupted by Iron Overload by Upregulating Wnt/Beta-Catenin Signaling. *Biomed. Res. Int.* 2020; 8256261.

54. Xu, W., Zhou, W., Cheng, M., Wang, J., Liu, Z., He, S., *et al.* (2017) Hypoxia activates Wnt/β-catenin signaling by regulating the expression of BCL9 in human hepatocellular carcinoma. *Sci. Rep.* 7; 40446.

55. Yamamoto-Fukuda, T., Aoki, D., Hishikawa, Y., Kobayashi, T., Takahashi, H. and Koji, T. (2003) Possible involvement of keratinocyte growth factor and its receptor in enhanced epithelial-cell proliferation and acquired recurrence of middle-ear cholesteatoma. *Lab. Invest.* 83; 123–136.

56. Yim, S. Y., Shim, J. J., Shin, J. H., Jeong, Y. S., Kang, S. H., Kim, S. B., *et al.* (2018) Integrated Genomic Comparison of Mouse Models Reveals Their Clinical Resemblance to Human Liver Cancer. *Mol. Cancer Res.* 16; 1713–1723.

57. Yoshii, A., Koji, T., Ohsawa, N. and Nakane, P. K. (1995) In situ localization of ribosomal RNAs is a reliable reference for hybridizable RNA in tissue sections. *J. Histochem. Cytochem.* 43; 321–327.

58. Zhang, S., Li, J., He, F. and Wang, X. M. (2015) Abnormal nuclear expression of Pygopus-2 in human primary hepatocellular carcinoma correlates with a poor prognosis. *Histopathology* 67; 176–184.

59. Zhu, R. X., Seto, W. K., Lai, C. L. and Yuen, M. F. (2016) Epidemiology of Hepatocellular Carcinoma in the Asia-Pacific Region. *Gut Liver*. 10; 332–339.